Nuclear Science and Techniques **23** (2012) 312–316

Reaction cross section studies of ^{12}C using the modified Glauber model in conjunction with nonlinear relativistic mean-field theory

FAN Guangwei[1,2] FUKUDA Mitsunori[3] AN Zhendong[1,2] CAI Xiaolu[1,2]
FAN Gongtao[1,2] HUANG Bosong[1,2] LI Yongjiang[1,2] XU Benji[1]
YAN Zhe[1,2] XU Wang[1,*]

[1]*Shanghai Institute of Applied Physics, Chinese Academy of Sciences, Jiading Campus, Shanghai 201800, China*

[2]*University of Chinese Academy of Sciences, Beijing 100049, China*

[3]*Graduate School of Science Faculty of Science, Osaka University, Osaka 560-0043, Japan*

Abstract We studied the structure of ^{12}C through the modified Glauber model using the density distributions calculated by the relativistic mean field theory. The experimental reaction cross sections of ^{12}C + ^{12}C were analyzed within the MOL by a χ^2–fitting procedure. The effects of the nuclear deformation on the reaction cross sections are studied. The reliable structure of ^{12}C is deduced. The studies show that the conjunction of these two models will be a more effective tool to study the properties of nuclei.

Key words Reaction cross section, RMF, Glauber model, nuclear density distribution

1 Introduction

The ^{12}C(α , γ)^{16}O reaction at low energies is considered to be the significant thermonuclear reaction in non-explosive helium burning. Its cross sections determine the ratio of ^{12}C/^{16}O at the end of the burning phase and affect the subsequent evolution and nucleosynthesis of massive stars up to their supernova explosion. But unfortunately, the measurement of the ^{12}C(α, γ)^{16}O reaction at He-burning energy $E_{c.m}$=0.3 MeV (center-of-mass=c.m.) is impossible now[1]. This necessitates theoretical extrapolations to the low energies of known measured cross sections from $E_{c.m}$>3 MeV. The structure of ^{12}C is relevant because it is the initial state for some theories during extrapolations, such as microscopic cluster model[2]. If the structure of ^{12}C is well determined, it will be much helpful for extrapolations.

The nuclear structure of ^{12}C has been intensively discussed theoretically, such as the shell model, the microscopic cluster model, the Hartree-Fock method and the relativistic mean-field (RMF) theory[3-5]. All of them can explain to vary degrees the experimental results of ^{12}C. Meanwhile, the structure of ^{12}C has been studied experimentally by electron scattering, monic atoms, β-NMR, proton scattering, etc. These methods provide good information for understanding the structure of ^{12}C[6,7]. In the mid-80s, radioactive nuclear beam technology was developed drastically. It has become possible to determine the nuclear structure for unstable nuclei. The study of the interaction between heavy ions becomes a major subject in the nuclear physics. Because a light heavy-ion and a stable nucleus, ^{12}C becomes a special interesting nucleus and has been used in many systems. Naturally, it becomes a calibration for many measurements[8].

In order to well study the structure of ^{12}C, we make an effort to study the reaction cross sections (σ_R) of ^{12}C + ^{12}C using the modified Glauber (MOL) in conjunction with the RMF theory. Because the RMF theory is successful in calculating the nuclear ground states[9] and the MOL is a powerful tool to explore the nuclear density distribution through σ_R[10], the conjunction of two models may be more sufficient to determine the nuclear structures. This may be a good

* Corresponding author. *E-mail address*: xuwang@sinap.ac.cn
Received date: 2011-03-17

attempt for this new Glauber model and the RMF theory. In this paper, we will describe briefly the formalism of the RMF and the MOL used in the present work in Sec.2. We will compare the σ_R of $^{12}C+^{12}C$ between experimental data and theoretical calculations in Sec.3. The conclusion will be given in Sec.4.

2 Formalisms of MOL and RMF

The Glauber model given by Glauber R J[11], which is based on the individual nucleon-nucleon collisions in the overlap zone of the colliding nuclei, successfully explained the observed σ_R at high energies. But it underestimates σ_R at low energies at least 10%[12], which causes an unreliable density distribution deduced by this method. Recently, it was modified by Abu-Ibrahim B and Suzuki Y[12] and Takechi, *et al*.[13] with including the multiple scattering effect and Fermi-motion effect respectively. The MOL could be able to explain σ_R at energy region from 30A MeV to 1A GeV for stable nucleus with uncertainties less than 2%[13]. It is well tested for unstable nucleus too and important achievements have been made on exotic nuclei of ^{22}C and ^{17}Ne by this method[14,15]. The MOL form for σ_R is expressed as:

$$\sigma_R = 2\pi\int_0^\infty b\mathrm{d}b[1-T(b)]C(E) \tag{1}$$

where $T(b)$ is the transmission as a function of the impact parameter b, the projectile pass through the target without interacting, and $C(E)$[16]denotes the influence of the Coulomb force. In the MOL calculation, $T(b)$ is expressed as:

$$T(b)=\mathrm{e}^{-2\mathrm{Im}\left\{\begin{array}{l}\frac{\mathrm{i}}{2}\int\mathrm{d}s\rho_z^{\mathrm{p}}(s)\{1-\exp[-\int\mathrm{d}t\rho_z^{\mathrm{T}}(t)\Gamma(b+s-t)]\}+\\ \frac{\mathrm{i}}{2}\int\mathrm{d}t\rho_z^{\mathrm{T}}(t)\{1-\exp[-\int\mathrm{d}s\rho_z^{\mathrm{p}}(s)\Gamma(b+t-s)]\}\end{array}\right\}} \tag{2}$$

where Γ is the profile function, ρ_z^{p} and ρ_z^{T} are the z-integrated densities of the projectile and the target nuclei, respectively, and s and t are the nucleon coordinates of the projectile and the target in the plane perpendicular to the beam axis. The profile function Γ is parameterized as

$$\Gamma(b)=\frac{1}{4\pi\beta}\sigma_{\mathrm{NN}}^{\mathrm{eff}}\exp(-\frac{b^2}{2\beta}) \tag{3}$$

where β is the so-called finite-range parameter, $\sigma_{\mathrm{NN}}^{\mathrm{eff}}$ is effective N-N cross section which is expressed as

$$\sigma_{\mathrm{NN}}^{\mathrm{eff}}=\int_{-\infty}^{+\infty}\mathrm{d}p_{\mathrm{rel}}\sigma_{\mathrm{NN}}(P_{\mathrm{rel}})D(P_{\mathrm{rel}}) \tag{4}$$

where $D(P_{rel})$ is the momentum distribution of a projectile nucleon relative to a target nucleon parallel to the beam axis (p_{rel}) in the frame of the Goldhaber model[17], which is expressed as,

$$D(p_{\mathrm{rel}})=\frac{1}{\sqrt{2\pi(\left\langle p^2\right\rangle^{\mathrm{p}}+\left\langle p^2\right\rangle^{\mathrm{T}})}}\times \exp[-(p_{\mathrm{rel}}-p_{\mathrm{proj}})^2/2(\left\langle p^2\right\rangle^{\mathrm{p}}+\left\langle p^2\right\rangle^{\mathrm{T}})] \tag{5}$$

where, $<P^2>^{\mathrm{P}}$ and $<P^2>^{\mathrm{T}}$ denote the mean-square momentum of the projectile and target nucleon, respectively, and p_{proj} is the momentum of a nucleon with the same velocity as the projectile nucleus.

This model requires the density distributions of the nuclei involved. In this calculation, the RMF-theory density distributions are mainly used as input density distributions, which have been extensively used for this purpose recently[18].

The RMF-theory which is based on the meson-exchange interactions, responsible for the saturation, and a strong spin-orbit force which is responsible for the magic numbers, has gained considerable success in describing various facets of nuclear structure properties. For instance, Furnstahl R J, *et al.*[19] have investigated magnetic moments of some nuclei, Marcos, Giai V, and Savushkin[20] have given Coulomb displacement energies in mirror nuclei, Ren Zhongzhou, *et al.*[21,22] predicted successfully neutron halo in O isotopes, the one-proton halo in ^{26}P and two-proton halo in ^{27}S by calculating the ground-state properties of them. Zhang Shisheng, *et al.*[23] explained the structure of ^{17}Ne. As a standard model, the starting point of the RMF theory is the Lagrangian density, which is written as:

$$\begin{aligned}L=&\bar{\boldsymbol{\Psi}}(\mathrm{i}\gamma^\mu\partial_\mu-M)\Psi-g_\sigma\sigma\Psi-g_\omega\bar{\boldsymbol{\Psi}}\gamma^\mu\omega_\mu\Psi\\&-g_\rho\bar{\boldsymbol{\Psi}}\gamma^\mu\rho_\mu^{\mathrm{a}}\vec{\boldsymbol{\tau}}^{\mathrm{a}}\Psi+\frac{1}{2}\partial^\mu\sigma\partial_\mu\sigma-\frac{1}{2}m_\sigma^2\sigma^3\\&-\frac{1}{4}g_3\sigma^4-\frac{1}{4}\vec{\boldsymbol{\Omega}}^{\mu\nu}\vec{\boldsymbol{\Omega}}_{\mu\nu}+\frac{1}{2}m_\omega^2\omega^\mu\omega_\mu-\frac{1}{4}\vec{\boldsymbol{R}}^{\mathrm{a}\mu\nu}\\&\times\vec{\boldsymbol{R}}_{\mu\nu}^{\mathrm{a}}+\frac{1}{2}m_\rho^2\rho^{\mathrm{a}\mu}\times\rho_\mu^{\mathrm{a}}-\frac{1}{4}\vec{\boldsymbol{F}}^{\mu\nu}\vec{\boldsymbol{F}}_{\mathrm{mn}}-e\bar{\boldsymbol{\Psi}}\gamma^\mu A^\mu\frac{1}{2}(1-\vec{\boldsymbol{\tau}}^3)\Psi\end{aligned} \tag{6}$$

with

$$\vec{\boldsymbol{\Omega}}^{\mu\nu} = \partial^{\mu}\omega^{\nu} - \partial^{\nu}\omega^{\mu} \tag{7}$$

$$\vec{\boldsymbol{R}}^{\alpha\mu\nu} = \partial^{\mu}\rho^{\alpha\nu} - \partial^{\nu}\rho^{\alpha\mu} + g_{\rho}\varepsilon^{abc}\rho^{b\mu}\rho^{c\nu} \tag{8}$$

$$\vec{\boldsymbol{F}}^{\mu\nu} = \partial^{\mu}A^{\nu} - \partial^{\nu}A^{\mu} \tag{9}$$

where the meson field are denoted by σ, ω_{μ} and ρ_{μ}^{α} and their masses are denoted by m_{σ} , m_{ω} and m_{ρ}, respectively. The nucleon field and rest mass are denoted by ψ and m. $A_{\mu.}$ is the photon field which is responsible for the electro-magnetic interaction $e^2/4\pi=1/137$. The effective strengths of the coupling between the mesons and nucleons are g_{σ}, g_{ω} and g_{ρ}, respectively. The g_2 and g_3 are the nonlinear coupling strengths of the σ meson. The isospin Pauli matrices are written as $\boldsymbol{\tau}^{a}$, $\boldsymbol{\tau}^{3}$ being the third component of $\boldsymbol{\tau}_{a}$. The third term in Eq.(8) is the strength tensor of the ρ field which is usually present only in gauge theories. Since the ρ field gives a small effect, it presumably has little consequence for the calculations. In practice the above parameters such as meson masses and coupling strengths are obtained through the fitting of the experimental observables which includes nuclear matter properties and binding energies and radii of a few selected spherical nuclei.

3 Calculations and discussions

In the present work, the σ_{R} of ^{12}C+^{12}C at different energies ranged from E_{Lab} = 30A MeV to 1GA MeV is studied using the MOL in conjunction with the RMF theory. The experimental finite-range parameter β [12] and the experimental momentum width $<P^2>^{1/2}$ of 90 MeV/c for projectile and target nucleus are employed in the MOL[13]. The numerical calculations of the RMF theory are carried out with force parameters: NL-SH, TM2, NL2 and NL3[24-27].

The numerical results of ^{12}C with NL-SH, TM2, NL2 and NL3 are listed in Table 1. In Table 1, R_{m}, R_{c}, R_{p} and R_{n} are the root-mean-square (RMS) radii of the matter, charge, proton and neutron distributions. The B is binding energy. It is seen from Table 1 that the difference of the theoretical radii and experimental one are only less than 4.2% and the radius using NL-SH parameter matches excellently with the experimental one. It indicates that the RMF theory is suitable for explaining the nuclear size and density profile of ^{12}C. However, the binding energies show us a different result. It causes troubles for us to determine the structure of ^{12}C, although this difference has been discussed theoretically several times[28].

Table 1 Comparison of experimental radius with calculations. The experimental R_{c} are normalized result from Ref.[29]. The experimental binding energy B is taken from Ref.[30].

	R_{m} (m-15)	R_{n} (m-15)	R_{p} (m-15)	R_{c} (m-15)	Expt. R_{c} (m-15)	B (MeV)	Expt. B (MeV)
NL-SH	2.446	2.296	2.318	2.456	2.464±0.009	89.58	92.16
TM2	2.481	2.334	2.355	2.491		92.86	
NL2	2.534	2.389	2.411	2.544		80.89	
NL3	2.350	2.200	2.216	2.360		91.15	

The calculations of the MOL directly clarify the difference and the structure of ^{12}C. Figure 1 shows us the σ_{R} of ^{12}C + ^{12}C. It clearly shows us that the calculation of the MOL with the RMF-theory density distribution using NL-SH parameter is more suitable for explaining the experimental σ_{R} than the calculations with the RMF-theory density distributions using other three parameters. The differences among the calculations are large to 16%. It indicates that the calculation of the MOL enlarges the difference between the radii. Figs.2 and 3 testify the reasonability of the conclusion. Fig.2 displays a reasonable relationship between the fit χ^2 and the difference of the calculations and experimental radius. The relationship should be the larger difference and the larger χ^2 or the worse fit. On the contrary, Fig.3 gives an unreasonable

relationship. This agrees with the theoretical discussions[22].

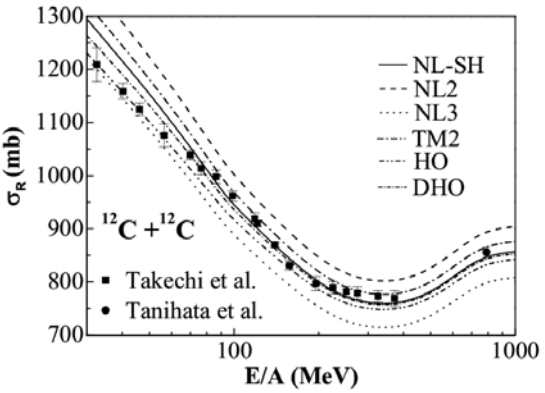

Fig.1 The σ_R data for $^{12}C+^{12}C$ as a function of beam energy. The solid squares are taken from Ref.[13], The solid circle is taken from Ref.[31]. The calculations are shown in curves.

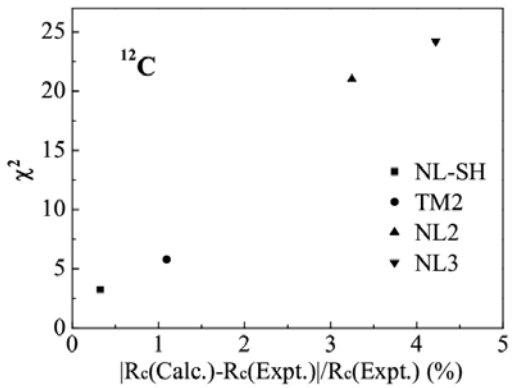

Fig.2 The analysis of the fit, which indicates the NL-SH is better for explaining the structure of ^{12}C than other three sets of parameters.

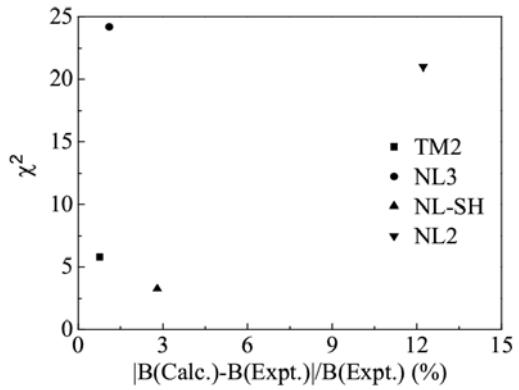

Fig.3 The relationship between the fit and the binding energy.

There are measurements suggest the ^{12}C have a large deformation structure. Such large deformation can affect the energy dependence of σ_R, therefore the effect should be studied in detail. We use the functional shape of harmonic oscillator (HO) function and the deformed harmonic oscillator (DHO) function as density distribution within the MOL calculation to study the effect[13]. The functional shapes are considered to be suitable for describing the density distribution of ^{12}C[8]. The HO function and DHO function are defined as follows:

$$\rho_{HO}(r) = \rho_{0(HO)} \times \left(1 + a\left(\frac{r}{b}\right)^2\right) \exp\left(-\left(\frac{r}{b}\right)^2\right) \quad (10)$$

$$\rho_{DHO}(r,\theta) = \int \rho_{0(DHO)} \left\{1 + a\left(\frac{r}{R(\theta)}\right)^2\right\} \exp\left[-\left(\frac{r}{R(\theta)}\right)^2\right] d\Omega \quad (11)$$

where $R(\theta)=R_0[1+\beta_2 Y_{20}(\theta)]$. The $\rho_{0(HO)}$ and $\rho_{0(DHO)}$ are normalization constants. The parameter a (=1.906 fm) and b (=1.538 fm) are determined through fits to the experimental RMS of charge by electron scattering and by unfolding the charge distributions. The R_0 (= 1.42 fm) and β_2 (= -0.623) are determined by fits to the experimental intrinsic quadrupole moments. The same a is used in two functions, because it affects the fit very small at about 1%, which can be neglected by comparing to the effects of R_0 (> 10%) and β_2 (> 10%). The calculations of σ_R are shown in Fig.1. The deformation effect increases calculated σ_R values less than 2%. This indicates the conclusion gotten above is reasonable.

4 Conclusion

The structure of ^{12}C is discussed by the utilization of the modified Glauber model in conjunction with the RMF theory. The experimental σ_R of ^{12}C + ^{12}C were analyzed within the MOL by a χ^2–fitting procedure. The fits show that the structure of ^{12}C can be well described by the RMF theory with NL-SH force parameter. On basis of the reasonable conclusion, the conjunction of these two models is helpful to precisely determine the nuclear structures. It can be a more effective tool to study the properties of the nuclei.

References

1 El Eid M F, Meyer B S. The L S Astrophys, 2004, **J611:** 452−465.

2 Dufour M, Descouvemont P. Phys Rev, 2008, **C**78, **015808:**1:11.

3 Chernykh M, Feldmeier H, Neff T*, et al.* Phys Rev Lett, 2007, 98, **032501:**1−4.

4 Amos K, Morrison I, Smith R, *et al.* Aust J Phys, 1981, **34:** 493−504.

5 Sugahara Y, Toki H. Nucl Phys, 1994, **A579:** 557−572.

6 Elton L R B. Nuclear Sizes. Oxford Univ (UK): London Press, 1961, 15−300.

7 Chaumeaux A, Layly V, Schaeffer R. Ann Phys, 1978, **116:** 247−357.

8 Ozawa A, Suzuki T, Tanihata I. Nucl Phys, 2001, **A693:** 32−62.

9 Horowitz C J Serot B D. Nucl Phys, 1981, **A368:** 503−517.

10 Takechi M, Fukuda M, Mihara M*, et al.* Eur Phys J, 2005, **A25:** 217−219.

11 Glauber R J, Lectures in theoretical Physics, Interscience (USA) 1959, **1:** 315−325.

12 Abu-Ibrahim B Suzuki Y. Phys Rev, 2000, C62, **034608:** 1−12.

13 Takechi M, Fukuda M, Mihara M, *et al.* Phys Rev, 2009, C79, **061601(R):** 1−9.

14 Tanaka K, Yamaguchi T, Suzuki T, *et al.* Phys Rev Lett, 2010, 104, **062701:** 1−4.

15 Tanaka K, Fukuda M, Mihara M, *et al.* Phys Rev, 2010, **C**82, **044309:** 1−10.

16 Fukuda M. Phys Lett, 1999, **B268:** 339−344.

17 Goldhaber A S, Phys Lett, 1974, **B53:** 306−310.

18 Patra S K, Panda R N, Arumugam P, *et al.* Phys Rev, 2009, **C**80, **064602:** 1−12.

19 Furnstahl R J, Price C E. Phys Rev, 1989, **C 40:** 1398−1406.

20 Marcos S, Giai Van N, Savushkin L N. Nucl Phys, 1992, **A549:** 143−152.

21 Ren Z Z, Mitting W, Chen B Q, *et al.* Phys Rev, 1995, **C52:** R20−R22.

22 Ren Z Z, Chen B Q, Ma Z Y, *et al.* Phys Rev, 1996, **C53:** R572−R575.

23 Zhang S S, Zhao E G, Zhou S G. http://arxiv.org/abs/1105.0504.

24 Sharma M M, Nagarajan M A, Ring P. Phys Lett, 1993, **B312:** 377−381.

25 Sharma M M, Lalazissis G A, Ring P. Phys Lett, 1993, **B317:** 9−13.

26 Reinhard P G. Rep Prog Phys, 1989, **52:** 439−455.

27 Reinhard P G, Rufa M, Maruhn M, *et al.* Zeitschrift für Physik A Hadrons and Nuclei, 1986, **A323**: 13−19.

28 Costa R S, Santiago A J. AIP Conference Proceedings, 2004, **1:** 473−479.

29 Fan G W, Xu W, Fukuda M*, et al.* Chinese Phys, 2010, **C34:** 1622−1627.

30 Audi G, Wapstra A H, Thibault C. Nucl Phys, 2003, **A729:** 337−676.

31 Tanihata I, Hamagaki H, Hashimoto. Phys Rev Lett, 1985, **55:** 2676−2680.